NANOSYSTEMS:
PHYSICS, CHEMISTRY, MATHEMATICS

Bykova E.N., et al. *Nanosystems: Phys. Chem. Math.*, 2026, **17** (1), 107–118.
http://nanojournal.ifmo.ru
DOI 10.17586/2220-8054-2026-17-1-107-118

Original article

Assessment of the effectiveness of 2D graphene structures derived from various biopolymers as modifiers of the properties of thermally stable polyimide films

Elena N. Bykova[1], Iosif V. Gofman[1], Igor V. Kuntsman[1], Elena M. Ivan'kova[1], Alexandr P. Voznyakovskii[2], Aleksei A. Vozniakovskii[3], Anna Yu. Neverovskaya[2]

[1]Branch of Petersburg Nuclear Physics Institute named by B.P. Konstantinov of National Research Centre "Kurchatov Institute" – Institute of Macromolecular Compounds, St. Petersburg, Russia

[2]Lebedev Institute of Synthetic Rubber, St. Petersburg, Russia

[3]Ioffe Institute, St. Petersburg, Russia

Corresponding author: E.N. Bykova, bykova.elena.n@gmail.com

PACS 62.25.-g, 65.80.Ck

ABSTRACT A comparative assessment of the influence of 2D graphene structures derived from lignin, starch and cellulose through the self-propagating high-temperature synthesis method on the mechanical, thermal and electrical properties of poly(4,4'-oxydiphenylene pyromellitimide) films was conducted. It was found that the incorporation of synthesized nanoparticles allows for the modification of the mechanical properties of the polyimide material without a significant decrease in volume and surface resistivity. Dependencies of the changes in properties of nanocomposite film materials on the following factors have also been established and analyzed: the type of biopolymer from which the nanofiller was obtained; the morphometric parameters of the prepared nanosized material; the concentration of the nanofiller.

KEYWORDS nanocomposites, 2D graphene structures, polyimides, biopolymers, mechanical properties, thermal properties

ACKNOWLEDGEMENTS This work was financially supported by the Russian Science Foundation (project No. 24-49-10014). The investigations of I.V. Gofman, I.V. Kuntsman, and E.M. Ivan'kova within this work were carried out within the state assignment of Branch of Petersburg Nuclear Physics Institute named by B. P. Konstantinov of National Research Centre "Kurchatov Institute" – Institute of Macromolecular Compounds (NRC "Kurchatov Institute" – PNPI – IMC). The authors of the article express their gratitude to the staff of the analytical laboratory of the NRC "Kurchatov Institute" – PNPI – IMC for conducting the elemental analysis of the synthesized nanoparticles.

FOR CITATION Bykova E.N., Gofman I.V., Kuntsman I.V., Ivan'kova E.M., Voznyakovskii A.P., Vozniakovskii A.A., Neverovskaya A.Yu. Assessment of the effectiveness of 2D graphene structures derived from various biopolymers as modifiers of the properties of thermally stable polyimide films. *Nanosystems: Phys. Chem. Math.*, 2026, **17** (1), 107–118.

1. Introduction

Many branches of modern industry increasingly require polymer materials that can maintain functionality under extreme operating conditions. Such materials include thermally stable aromatic polyimides (PIs), which combine record-high mechanical, thermal, and dielectric properties and exhibit high hydrolytic and radiation resistance [1,2]. Due to these properties, PIs find wide applications in various engineering fields as thermally and chemically resistant electrical insulation films [1,2] and protective coatings [3], as well as in structural materials with high mechanical performance [1,2]. However, despite significant advancements in the synthesis of polyimide materials, their most critical performance characteristics, such as mechanical stiffness, thermal stability, heat resistance and others, need further improvement. Modifying the polymer matrix with high dispersity fillers is the most promising approach for obtaining polymer materials with improved physicochemical and physico-mechanical properties, leading to the development of composite materials [4–8]. This trend is based on a phenomenological model that suggests that nano-dispersed particles within the polymer matrix influence not a single specific parameter (most commonly referred to as mechanical stiffness) of the polymer material but rather affect a complex set of its physicochemical parameters [6–8].

Theoretical methods, particularly all-atomistic molecular-dynamics simulations [9–11], allow for a reasonably accurate prediction of the trends regarding the influence of nanoparticles on the polymer matrix and the revealing of matrix parameters which will change most significantly depending on the nature, architecture, and dispersity of the nanoparticles. However, these methods require verifying the models used against experimental data and comparing simulation results

with experimental findings. Thus, the selection of nanoparticles as fillers to enhance a specific performance parameter or a set of parameters largely depends on the experimenter's intuition and experience. It is important to note that each case is unique, and extensive experimental testing and optimization may be required to achieve the desired results.

Among the various types of nanoparticles, 2D graphene structures (graphene oxide, reduced graphene oxide, graphene-modified in multiple ways, etc.) are of particular interest because many structures of this type possess the unique properties, such as high mechanical stiffness, electrical conductivity, and thermal conductivity [12, 13]. Research shows [14–18] that, due to the unique characteristics of graphene nanoparticles, their incorporation into a polymer matrix leads to improvements in the nanocomposite material's mechanical, thermal, anti-corrosive, and tribological properties.

However, despite the apparent advantages, the widespread use of graphene nanostructures is limited by several factors. The first is the high cost of graphene structures and the low productivity of most existing methods for their production. The second important factor is the potential environmental hazards associated with most known methods of synthesizing graphene nanostructures of industrial output, which arise from using aggressive acidic and alkaline agents to process the starting graphite. The third factor is the tendency of graphene structures to aggregate when introduced into polymer solutions and melts [19]. In this regard, there is currently active research aimed at developing more cost-effective and safer methods for the production of graphene nanostructures and optimizing the methods and conditions for surface treatment of these nanoparticles prior to their incorporation into the polymer matrix. These efforts aim to reduce nanoparticle aggregation and enhance their interaction with the polymer matrix.

One of the promising methods is a recently developed approach for the production of graphene nanostructures through the carbonization of biopolymers of plant origin (lignin, cellulose, starch, and glucose) [20], as well as plant biomass in the form of tree bark [21] and hogweed [22], under the conditions of a self-propagating high-temperature synthesis (SHS) process. The SHS method refers to the process of the propagation of a spin wave of a strongly exothermic reaction through a mixture of reagents (oxidizer and reducer), in which heat release is localized in a layer and transferred from layer to layer via heat conduction through a branched-chain ignition mechanism [23].

In contrast to thermal ignition, branching chain ignition is caused by the avalanche multiplication of active intermediate products (free atoms, radicals, and sometimes excited particles) in their rapid reactions with the initial reagents and among themselves. This mechanism ensures the realization of the reaction in a narrow zone that propagates through the material due to heat transfer following the local initiation of the response in a layer of cold reagent mixture that is not subjected to volumetric heating. Regarding performance and environmental safety, SHS fully meets the requirements imposed on modern technologies. It should be noted that our synthesis method of graphene structures refers to "bottom-up" processes. In other words, at the first stage, the initial biopolymer (precursor) is destroyed to low-molecular products due to thermo-oxidative SHS processes. Subsequently, these products form 2D graphene structures, namely particles of few-layer graphene (FLG), due to self-organization processes.

Considering this circumstance, it can be assumed that the use of "traditional" methodologies based on various mechanisms for obtaining graphene structures "top-down" (in particular, the Hummers method [24]) and "bottom-up" approaches (specifically, the SHS method proposed by us) will lead to graphene structures that differ in a range of characteristics, such as the defectiveness of graphene layers, including Stone–Wales defects [25]; the polydispersity parameters of graphene particles; and the nature and quantity of functional groups. Consequently, the differences in the morphometric parameters of graphene particles synthesized through different mechanisms and using various precursors may also influence the nature of their interaction with the polymer matrix.

Thus, although our proposed synthesis method offers advantages in terms of productivity and environmental friendliness compared to methods based on the exfoliation of graphene layers from natural graphite, its use as an alternative to "traditional" graphene production methods requires experimental validation of the quality of the obtained products. This work's objectives included the characterization of the properties of FLG nanoparticles obtained by the SHS method from various biopolymers and the investigation of the possibilities for modifying the properties of thermally stable polymer films by incorporating the synthesized nanoparticles. The matrix polymer film material selected is aromatic PI – poly(4,4'-oxydiphenylene pyromellitimide) (PMDA-ODA) [1, 2], which is widely used in various fields of engineering, primarily as heat-resistant dielectric materials with high mechanical properties.

2. Materials and methods

2.1. Materials

The structure of the matrix polymer PMDA-ODA is as follows:

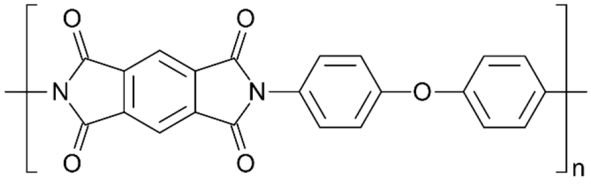

The solution of polyamic acid (PAA) in N-methylpyrrolidone (concentration 15 wt %) – the polymer-precursor of PI PMDA-ODA was obtained from Sigma-Aldrich (product No. 575828). N-methylpyrrolidone (chemically pure) was obtained from Vekton (Russia). Ammonium nitrate (chemically pure) and isopropyl alcohol (chemically pure) were acquired from Lenreaktiv (Russia). As precursors for the synthesis of graphene structures, lignin, microcrystalline cellulose, and starch were selected. Lignin was extracted from the black liquor of industrial cooking processes at Mondi SLPK joint-stock company (Russia) by treating the partially evaporated black liquor with sulfuric acid (10 wt. %) at a temperature of 60 °C until a pH of 4 was reached. The precipitate was washed with distilled water until a neutral pH was achieved and then dried at a temperature of 35 – 40 °C. Removal of low-molecular-weight organic impurities was carried out by extraction with diethyl ether. The carbonized product obtained from lignin by means of SHS is designated as FLG-1. Starch and microcrystalline cellulose were obtained from Aptechny Sklad Khimfarmprodukt Co (Russia); their carbonized products are designated as FLG-2 and FLG-3, respectively. As a reference sample, graphene supplied by Sigma-Aldrich (product cat. No. 900394, Merck, Germany) was used – FLG-0. The particle size of FLG-0 is < 2 μm and the specific surface area is 300 m^2/g.

2.2. Synthesis of FLG

The synthesis of FLG was carried out according to the methodology previously developed by the authors [20–22]. Before use, all biopolymers underwent preliminary treatment: they were dried, ground and sieved to obtain a homogeneous mass. Then, the prepared samples were mixed with the oxidizer powder in a mass ratio of biopolymer to oxidizer = 1:1. In this study, ammonium nitrate was used as the oxidizer. The resulting reaction mixture was placed in a glass flask that was immersed in an oil bath heated to 220 °C. In the course of the reaction, significant gas evolution was observed; the termination of this gas evolution indicated the completion of the SHS process. The obtained powder was washed with hot distilled water and isopropyl alcohol and then the solvent was removed under vacuum at 280 °C.

2.3. Films preparation

A two-stage synthesis method was used to prepare the control and nanocomposite films [1, 26, 27]. At the first stage of synthesis, a soluble polymer-precursor – PAA was obtained (this stage was carried out by Sigma-Aldrich). The layers of PAA solutions were cast onto flat glass plates using a template and dried in a thermostat at a temperature of 80 °C for 4 hours. Then, to obtain PIs, the PAA films were cyclized by heating on the substrate in an oven at a rate of 3 °C/min up to 360 °C, followed by a hold at this temperature for 30 minutes. The composite films were prepared using a standard solution processing technique. The calculated amount of nanoparticles were subjected to thermal treatment for 1 hour at 100 °C to remove the residual water sorbed during the storage, after which these nanoparticles were dispersed in N-methyl pyrrolidone using an ultrasonic disperser. The obtained dispersion was combined with the PAA solutions, followed by homogenization of the mixture through prolonged stirring (24 hours) using a top-driven mechanical stirrer at 1000 rpm. Nanocomposite films based on PI were produced from the homogenized mixtures using the methodology described above.

2.4. Characterization techniques

The electron micrographs of the carbonized products were obtained using a Zeiss Libra 200FE transmission electron microscope (ZEISS, Germany) at 50 kV. The morphology of the FLG-1 to FLG-3 samples, as well as the nanocomposite film materials based on them, was investigated using a SUPRA-55VP scanning electron microscope (SEM) (Carl Zeiss, Oberkochen, Germany). The samples were mounted on the microscope holders using a special adhesive. To study the morphology and assess the charge dissipation properties of the FLG particles, they were intentionally left uncoated, forgoing the standard platinum sputtering procedure. X-ray diffraction (XRD) analysis of the samples was conducted using an XRF-1800 spectrometer (Shimadzu, Japan). The measurement was performed on a pressed pellet consisting of the investigated material and polyvinyl alcohol (as a binder) on a boric acid substrate. Pressing was carried out using a Carber 3912 tool. Raman spectra were obtained using a Horiba Yobin Yvon LabRam HR 800 spectrometer (532 nm laser, 1800 lines/mm diffraction grating, microscope with x20 magnification). Infrared absorption spectra were recorded using the InfraLUM FT-08 spectrometer (Lumex, Russia). The elemental analysis of nanoparticles samples obtained by the SHS method was performed using a CHN Vario EL III elemental analyzer (Elementar Analysensysteme GmbH, Germany). The specific surface was measured using ASAP 2020 MR (Micromeritics, USA) by the BET method. Nitrogen was used as the adsorbate gas. Before the measurement, the samples were held for 2 h in vacuo at 300 °C. True density was measured using gas (helium) pycnometry on the Ultrapycnometer 1000 instrument (Quantachrome Instruments, USA).

The thermal characteristics of the FLG-1 to FLG-3 samples, as well as the nanocomposite film materials containing these nanoparticles, were investigated using simultaneous thermogravimetric (TGA) and differential thermal (DTA) analyses in a static air environment with a DTG-60 analyzer (Shimadzu, Japan). The heating rate of the samples was set at 5 °C/min. Based on the analysis results, the temperature at which the destruction process is completed ($T_{\text{full dest}}$), beyond which the sample mass remains unchanged and the coke residue (m_{fin}/m_0) were determined. Additionally, the temperatures corresponding to the onset of thermal degradation (τ_0) and the temperatures at which the sample mass decreases by 1, 5 and 10 % (τ_1, τ_5 and τ_{10}, respectively) were calculated. Furthermore, the temperature at which the maximum rate of mass loss was recorded ($T|_{dm/dT\,\max}$) was determined from the first derivative of the mass loss curve (DTG). The

glass transition temperatures (T_g) of the PI-based nanocomposite film samples were determined using thermomechanical analysis (TMA) with a TMA 402 F1 Hyperion apparatus (NETZSCH, Germany). The tests were performed in a uniaxial stretching mode under a constant tensile force of 0.5 MPa while the sample was heated at a steady rate of 5 °C/min in an argon atmosphere.

The mechanical tests of the films were conducted at room temperature in a uniaxial stretching mode using a universal testing machine, Autograph AGS-X 5 kN (Shimadzu, Japan). The samples, with a working size of 20×2 mm, were tested at a stretching rate of 10 mm/min. During the tests, the following material properties were determined: Young's modulus (E), yield stress (σ_y) (in cases where it could be achieved during the sample stretching), break stress (σ_b) and ultimate deformation (ε_b). For each tested material, average values and standard deviations were calculated based on measurements taken from 6 – 9 fragments of the material. The values of the matrix and composite films' volume and surface electrical resistivity were determined using a two-electrode method on a teraohmmeter E6-A13 (Metromex, Russia). The samples were placed in a specially designed circular cell connected to the electrodes. To eliminate surface leakage current during the measurement of the samples' volume electrical resistivity, a special guard ring surrounding the measuring circular electrode was employed, this ring was grounded during the measurement. When measuring the surface electrical resistance with the given electrode configuration, the voltage is applied between the guard ring and the central electrode, the bottom electrode being grounded. The values of the volume and surface resistances of the dielectric sample were determined under a constant voltage of $U = 100$ V using the following formula.

$$R_{V(S)} = \frac{U}{I_{V(S)}}, \tag{1}$$

where $I_{V(S)}$ is the current flowing through the volume or along the surface of the sample after the charge transfer process has reached equilibrium. The volume resistivity of the material was determined using the following formula:

$$\rho_V = \frac{R_V \cdot S}{h} = \frac{U \cdot S}{I_V \cdot h}, \tag{2}$$

where I_V is the measured volume current; U is the voltage across the electrodes; S is the area of the central measuring electrode; h is the thickness of the dielectric; and R_V is the volume resistance of the sample. The surface resistivity can be calculated using the following formula:

$$\rho_S = \frac{R_S \cdot \pi \cdot (d_1 + d_2)}{d_1 - d_2}, \tag{3}$$

where R_S is the surface electrical resistance of the dielectric sample confined between the electrodes; d_1 is the inner diameter of the guard ring; and d_2 is the diameter of the central electrode.

3. Results and discussion

Earlier, we demonstrated that the carbonization of natural biopolymers under the conditions of the self-propagating high-temperature synthesis process leads to the formation of 2D graphene structures, which are promising for use as modifying additives in polymer matrices [28]. In this study, three types of biopolymers were chosen as precursors: starch, microcrystalline cellulose, and sulfonated lignin. These biopolymers significantly differ in the architecture of their macromolecular chains [29, 30]. Consequently, one could expect differences in the morphometric parameters of the final FLG.

3.1. Characterization of carbonized products

The carbonized products were studied using a combination of complementary methods, such as electron microscopy, Raman and FTIR spectroscopy, and X-ray diffraction analysis. The density and specific surface area values of these samples were also determined. The morphology of the SHS-synthesized FLG was characterized by SEM and TEM (Fig. 1). As was established in our earlier studies, the lateral dimensions of the synthesized nanoparticles reached up to 0.2 – 0.3 μm [31]. The analysis of the TEM images presented in Fig. 1(a–c) showed that the particles of powders FLG-1 to FLG-3 have a leaf-like shape with varying degrees of transparency. Since each individual monolayer particle is transparent, the presence of darker areas can be explained by multiple graphene sheets in the stack. Furthermore, the chaotic distribution of transparent and dark regions may indicate that the resulting particles have a curved surface, meaning they are "scaly" particles, characteristic of 2D carbon structures [32].

SEM analysis revealed a pronounced dependence of morphology and charge dissipation behavior on the nature of the precursor. While all synthesized samples exhibited some degree of charge accumulation, FLG derived from lignin (Fig. 1(d)) and cellulose (Fig. 1(f)) demonstrated a highly ordered platelet-like structure with relatively minimal defectivity and showed the most effective charge dissipation among them. In contrast, the analogues obtained from starch (Fig. 1(e)) exhibited a severely disrupted structure composed of defective platelets along with a significantly higher propensity for charge accumulation, indicating their inferior electrical conductivity.

The Raman scattering data presented in Fig. 2 demonstrate four peaks: 1355 – 1365 cm^{-1} (D), 1574 – 1595 cm^{-1} (G), 2730 – 2760 cm^{-1} (2D), and 2930 – 2960 cm^{-1} (D+G). The D peak corresponds to a defect in the sp^2 lattice, while the G peak is associated with sp^2 hybridized carbon. The overall shape of the resulting Raman spectra of the carbonized

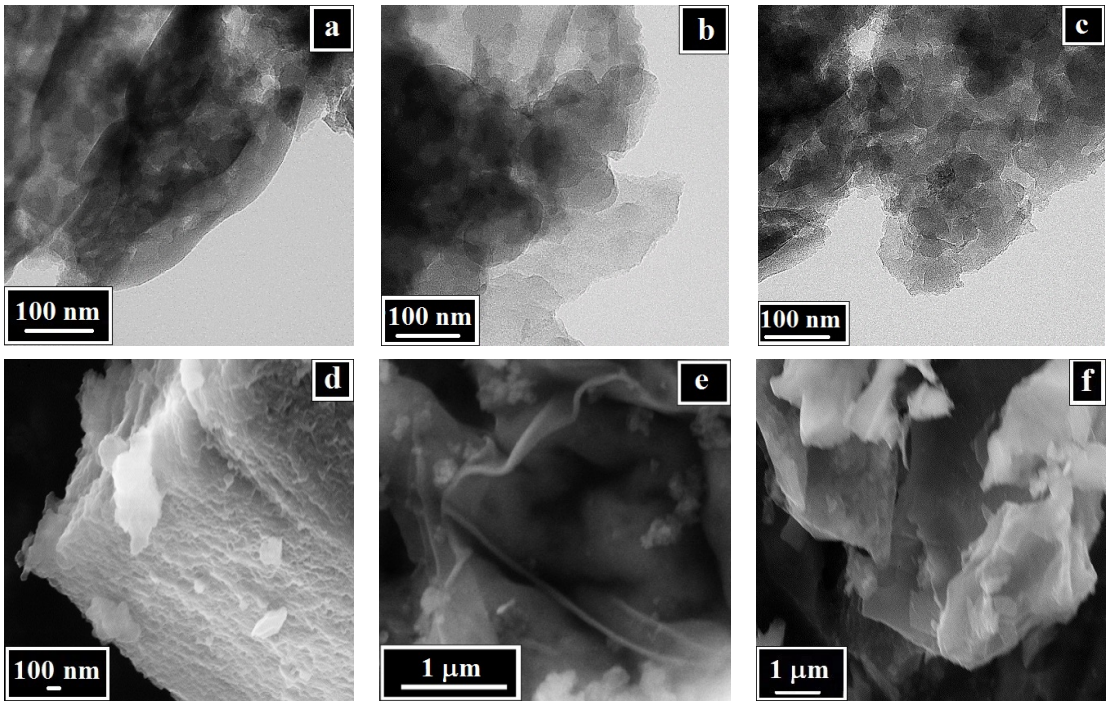

FIG. 1. TEM (a–c) and SEM (d–f) images of samples FLG-1 (a, d), FLG-2 (b, e), and FLG-3 (c, f)

products align with the spectral characteristics of 2D graphene structures [33, 34]. The defectiveness of the synthesized FLG samples can be assessed by the intensity ratio of the D and G peaks. A ratio close to 1 indicates a high level of defectiveness in the obtained samples. Comparing the Raman scattering data for the synthesized FLG samples, it can be concluded that FLG-1 ($I_D/I_G = 0.62$) is characterized by the lowest defectiveness, while FLG-2 ($I_D/I_G = 0.97$) exhibits the highest defectiveness.

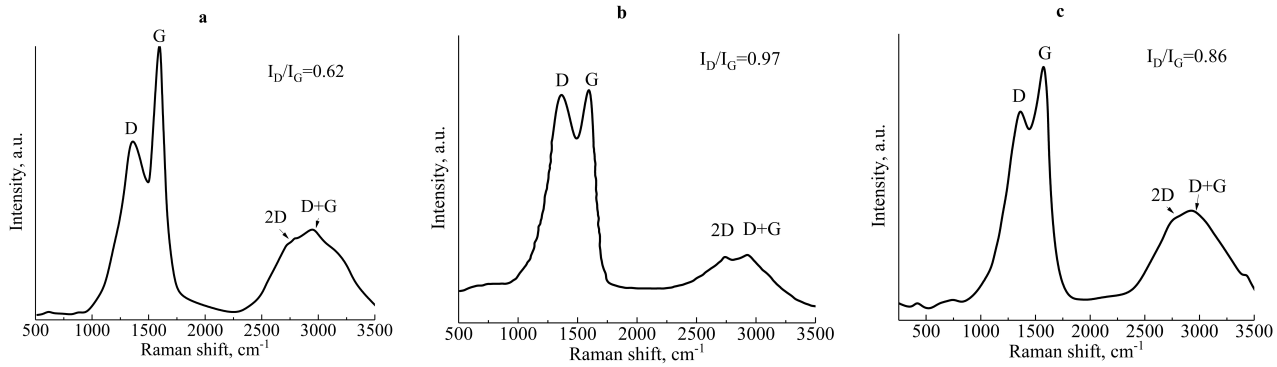

FIG. 2. Raman spectra of FLG-1 (a), FLG-2 (b), FLG-3 (c) samples

Let us note that the nature of the precursor determines not only the defectiveness of the synthesized FLG but also its specific surface area and density (Table 1).

TABLE 1. Specific surface area and density of samples FLG-1, FLG-2 and FLG-3

FLG-1	FLG-2	FLG-3
Density, g/cm^3		
2.011	1.910	1.975
Specific surface area, m^2/g		
590	436	621

The synthesized FLG particles differ somewhat in properties from commercially available graphene structures obtained through the most commonly used methods. For example, (Fig. 3), in addition to the C–H, C–OH, CO–C, and C=C bonds characteristic of graphene structures, the synthesized particles also exhibit a C–N bond, indicating the presence of nitrogen-containing groups in the FLG obtained by this method. The presence of these groups is due to the use of ammonium nitrate as an oxidizer.

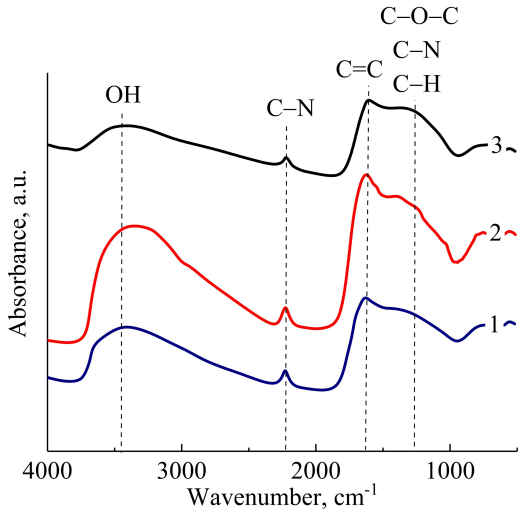

FIG. 3. IR spectra of samples FLG-1 (1), FLG-2 (2) and FLG-3 (3)

The results of the elemental analysis conducted on a CHN analyzer in this study showed that the concentration of nitrogen atoms in the synthesized FLG significantly depends on the type of precursor: in the samples FLG-1, FLG-2, and FLG-3, the nitrogen content is 7.75, 14.60, and 15.19 %, respectively. XRD was conducted to demonstrate the absence of graphite structures other than FLG, namely graphite, thermally expanded graphite, graphene oxide in the obtained materials. The X-ray diffraction pattern of the FLG-3 sample is presented in Fig. 4 as an illustration.

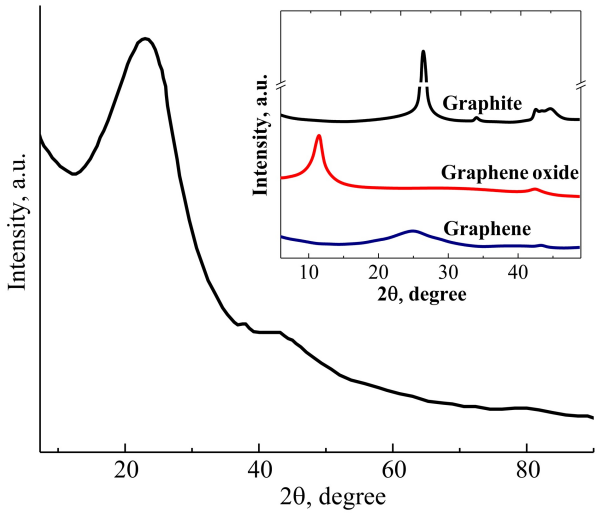

FIG. 4. X-ray diffraction pattern of the FLG-3. For comparison, the insert shows the X-ray diffraction patterns of graphite, graphene oxide, and graphene obtained in the study [35]

The presence of only two halos in the range of 10 to 35 degrees and in the area from approximately 43 to 50 degrees without any sharp diffraction peaks demonstrates the absence of any graphite regions in the material (Fig. 4), whose diffraction is characterized primarily by a narrow and intense peak at around 26 degrees, as well as a narrow peak with low intensity in the range of 54 – 55 degrees [35, 36].

3.2. Thermal analysis of samples FLG-1 to FLG-3

The results of the combined thermal analysis TGA and DTA, presented in Table 2 and Fig. 5, show that upon heating samples FLG-1 to FLG-3 from room temperature to 100 – 120 °C, a significant mass loss (5 – 10 %) was observed,

accompanied by the appearance of an endothermic peak on the DTA curves, with a maximum at 65 – 70 °C. This phenomenon undoubtedly corresponds to the removal of water adsorbed on the surface and/or within the volume of the particles. This effect is likely attributed to the presence of hydrophilic oxygen-containing functional groups on the surfaces of the synthesized materials and their relatively loose and porous structure (Table 1).

After the onset of thermal degradation, the process rate increases monotonically with rising temperature, reaching a maximum value in the range of 482 – 524 °C. In the same temperature region, an exothermic thermal effect is observed on the DTA curves, with maxima at 475 – 526 °C.

TABLE 2. Thermal characteristics of samples FLG-1 to FLG-3

Sample	τ_0, °C	τ_1, °C	τ_5, °C	τ_{10}, °C	$T\|_{dm/dT\ \max}$, °C	$T_{\text{full dest}}$, °C	m_{fin}/m_0, %
FLG-1	245	281	332	364	482	580	4.47
FLG-2	205	235	281	308	524	550	1.93
FLG-3	275	316	373	403	494	595	2.24

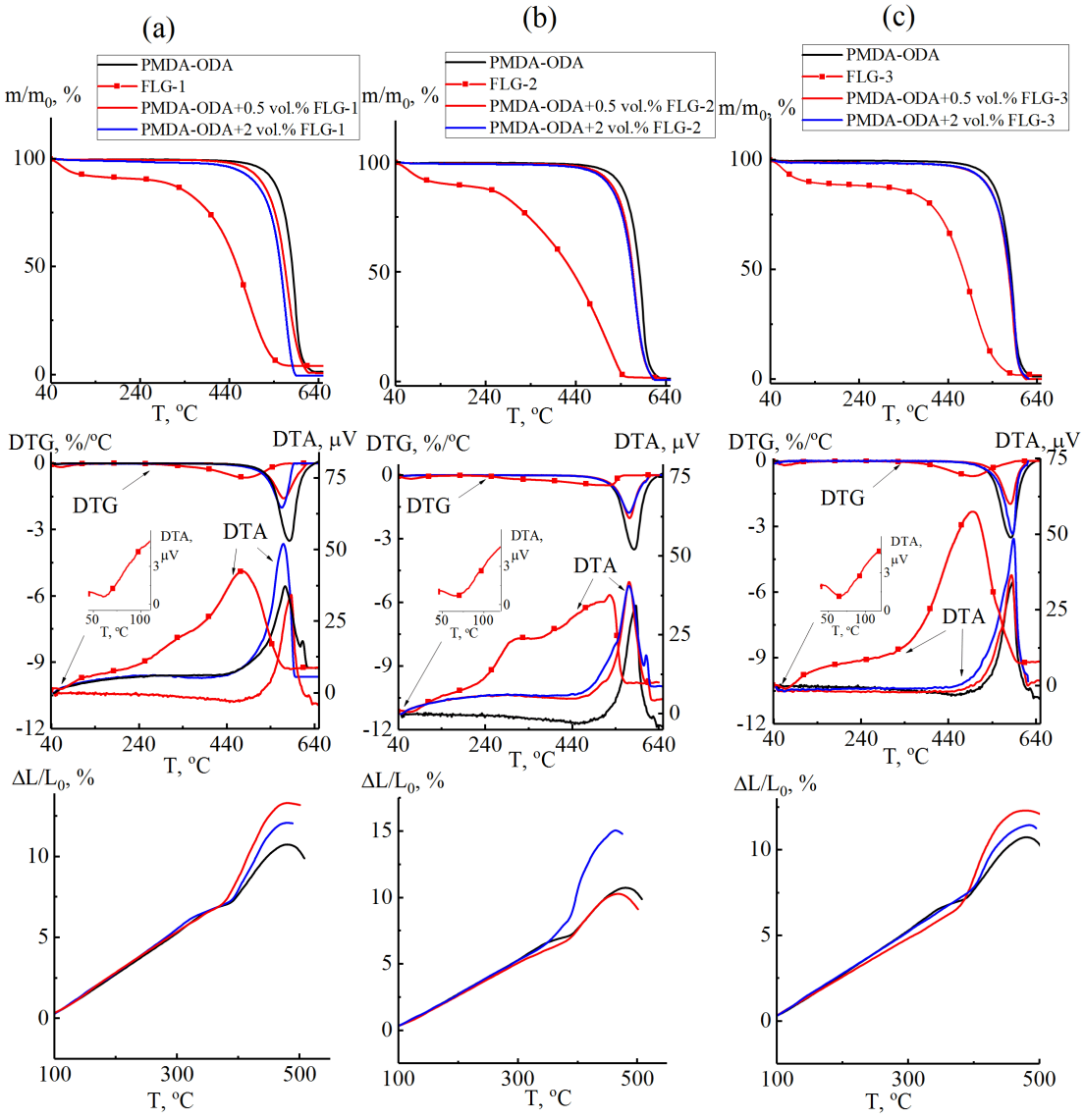

FIG. 5. TGA, DTG, DTA and TMA curves of matrix and composite films of PMDA-ODA containing 0.5 and 2 vol. % FLG-1 (a), FLG-2 (b) and FLG-3 (c). Inset: DTA curves of the samples in the temperature range of 40 – 120 °C

The depression of mass of all the FLG samples studied during the TGA process was completely stopped up to the temperatures range of 550 – 595 °C (Fig. 5). The further heating of the samples did not provoke any additional fall of their mass (in the control experiments we have tested the mass in the heating process up to 800 °C. It is well known that even heat-resistant polymer materials completely degrade in air, forming volatile compounds in a temperature range up to ∼ 600 °C [37]. This is all the more true for thermo-oxidative destruction processes of biopolymers and their reprocessing products. Thus, it can be concluded that the residual mass of the sample (1.93 – 4.47 %) recorded in our experiments when heating FLG above 600 °C refers to inorganic impurities present in the samples. The experimental methods at our disposal do not allow to specify the elemental composition of these impurities, but they can reliably estimate their amount in studied FLG.

It should be noted that the thermal stability of FLG is determined by the type of biopolymer used for its synthesis. The data presented in Table 2 show that the sample FLG-3, synthesized from cellulose, demonstrates the highest thermal stability. These particles exceed FLG-1, obtained from lignin, by 39 °C in terms of τ_{10}, and FLG-2, synthesized from starch, by 95 °C. The observed differences in thermal stability are likely related to the varying content of oxygen-containing and nitrogen-containing functional groups in the synthesized materials.

It can be hypothesized that the enhanced thermal stability observed for the FLG-3 sample is largely attributable to a lower content of oxygen-containing functional groups and a higher abundance of nitrogen-containing functional groups compared to the FLG-1 and FLG-2 samples. The elemental analysis data support this hypothesis presented earlier, as well as the DTA results depicted in Fig. 5. In contrast to FLG-3, the DTA curves of FLG-1 and FLG-2 samples exhibit an additional exothermic thermal effect within the temperature range of 240 to 370 °C, with a maximum at 300 °C, which may be indicative of the removal of oxygen-containing functional groups from the graphene structure [38].

3.3. Thermal analysis of nanocomposite film samples

The results of TGA and DTA, presented in Fig. 5 and Table 3, indicated that incorporating all types of FLG particles used in the work does not qualitatively affect the thermal degradation processes of the polyimide material. For both the control film PMDA-ODA and the composite films, the thermal degradation process begins in the range of approximately 400 – 460 °C, with the maximum degradation rate occurring at around 570 – 590 °C, and this process is finished in the range of roughly 590 – 630 °C. The incorporation of nanoparticles of all types into PMDA-ODA films generally resulted in a certain reduction in thermal stability metrics. Such an effect was anticipated, as the TGA results (Fig. 5, Tables 2 and 3) indicate lower thermal stability values (up to τ_{10}) for the nanoparticles themselves compared to the thermal stability of the PI matrix.

The TMA results are presented in Fig. 5 and Table 3. The incorporation of synthesized nanoparticles into the PI matrix generally decreases the material's glass transition temperature. It is noteworthy that, in some cases, this reduction was accompanied by an increase in the films' flexibility beyond the glass transition (Fig. 5). The most likely reason for this effect is the formation of excess free volume in the polymer material due to the aggregation of the synthesized nanoparticles. However, the PMDA-ODA film sample containing 2 vol. % FLG-3 was an exception: the glass transition temperature of the nanocomposite film increased by 11 °C compared to the unfilled sample. This is likely attributed to additional interactions between the surface groups of FLG-3 and the matrix polymer. It appears that such interactions, despite the significant aggregation of these nanoparticles, may hinder the segmental mobility of the polymer chain and slightly increase the glass transition temperature of the composite material.

TABLE 3. Thermal characteristics of PMDA-ODA matrix films and PMDA-ODA-based composite materials

Sample	T_g, °C	τ_5, °C	τ_{10}, °C	$T\|_{dm/dT\,\max}$, °C
PMDA-ODA	391	523	540	584
PMDA-ODA+0.5 vol. % FLG-1	382	493	516	570
PMDA-ODA+2 vol. % FLG-1	390	476	502	564
PMDA-ODA+0.5 vol. % FLG-2	387	501	524	572
PMDA-ODA+2 vol. % FLG-2	384	498	520	570
PMDA-ODA+0.5 vol. % FLG-3	385	512	532	582
PMDA-ODA+2 vol. % FLG-3	402	508	529	586

3.4. Mechanical properties

It is well known [39] that the positive influence of nanosized fillers on the mechanics of polymer film materials primarily manifests as reinforcement of the matrix material, leading to an increase in its stiffness. This results in a growth

of Young's modulus and, to a lesser extent, the material's yield stress. As for the strength characteristics, increasing the material's strength is quite rare in this context. As a rule [39], an increase in the concentration of nanoparticles increases the material's stiffness, accompanied by a significant decrease in strength and ultimate deformation. Researchers often attribute this effect to the heterogenization of the material's structure and the emergence of additional stresses at the phase boundaries of the "polymer matrix – nanoparticles". However, this decrease in break stress and ultimate deformation is not critical when considering the situation from the perspective of practical material usage. Indeed, for most polymer film materials, including the PMDA-ODA matrix, failure occurs at relatively large deformations, where these deformations are inherently irreversible. Thus, the actual magnitude of deformations permissible during the material's service life does not exceed a few percent. It is precisely within this range that the reinforcement effect manifests quite significantly, provided it can be achieved by incorporating nanoparticles.

For composite films filled with the studied nanoparticles, the realization of the aforementioned reinforcement effect within certain limits can be stated (Table 4). A slight (11 %) increase in Young's modulus was achieved by incorporating 2 vol. % of FLG-1 particles into the PMDA-ODA matrix. A less pronounced increase in the modulus (6 %) was observed with the introduction of 2 vol. % of FLG-2 into the polymer. The same increase in Young's modulus was recorded with the addition of 0.5 vol. % of FLG-3; however, further increasing the concentration of these nanoparticles caused the modulus to drop below the value characteristic of the unfilled film. Finally, as expected, introducing all the nanoparticles used in this study led to a consistent decrease in the ultimate deformation and, consequently, the break stress of the material as their concentration increased.

TABLE 4. Mechanical properties of PMDA-ODA matrix films and PMDA-ODA-based composite materials

Sample	E, GPa	E/E_0	σ_y, MPa	σ_b, MPa	ε_b, %
PMDA-ODA	2.85±0.11	1.00	96±3	149±12	63±4
PMDA-ODA+0.5 vol. % FLG-1	3.06±0.09	1.07	97±1	125±5	30±2
PMDA-ODA+2 vol. % FLG-1	3.15±0.07	1.11	106±3	128±2	27±1
PMDA-ODA+0.5 vol. % FLG-2	2.92±0.06	1.02	104±1	131±1	41±3
PMDA-ODA+2 vol. % FLG-2	3.03±0.09	1.06	103±3	126±2	27±1
PMDA-ODA+0.5 vol. % FLG-3	2.99±0.06	1.05	96±2	112±6	25±6
PMDA-ODA+2 vol. % FLG-3	2.79±0.14	0.98	—	98±6	17±3

E_0 – Young's modulus of the PMDA-ODA matrix polymer film

Summarizing this part of the research, it can be concluded that the most effective modifier of the PI mechanical properties is the FLG-1 material. Its superiority is directly due to its optimal dispersibility within the polymer matrix and minimal tendency to agglomerate, which is confirmed by SEM analysis data (Fig. 6).

In contrast to FLG-1 (Fig. 6(a,d)), the composites with FLG-2 (Fig. 6(b,e)) and FLG-3 (Fig. 6(c,f)) form significantly larger and more numerous agglomerates. These structures act as stress concentrators, leading to a consequent deterioration in the material's strength characteristics. The greatest propensity for aggregation is observed in FLG-3 particles, which is consistent with previously published data [20] and explains the most substantial decline in mechanical properties precisely in this nanocomposite.

3.5. Dielectric properties

As is known [40] and demonstrated by the example of PMDA-ODA films containing commercially available graphene FLG-0, the introduction of carbon nanoparticles, even in small concentrations, can significantly increase the electrical conductivity of polymer materials (Table 5). Considering PI films' primary application area, this sharply narrows their practical application range. Therefore, it was imperative to evaluate how introducing synthesized nanoparticles affects the dielectric properties of PI films.

Based on the data from Table 5, it is evident that the nanocomposite films containing the synthesized nanoparticles exhibit high values of volume and surface resistivity, corresponding to these materials' low electrical conductivity. Since the electrical conductivity of such nanocomposite materials filled with carbon nanoparticles is realized through the movement of charge carriers across the filler particles, it is most likely that the observed effect is due to the presence of functional groups on the surface of the synthesized nanoparticles [41, 42]. These groups contribute to blocking electrical contacts between the conductive nanoparticles, meaning there are no continuous electrical pathways within the material, known as the percolation cluster, which directly affects the conductivity of the nanocomposite polymer material. For nanocomposites filled with control graphene particles (FLG-0), the effect of blocking contacts between nanoparticles is not observed, which suggests the absence of any non-conducting groups on their surface.

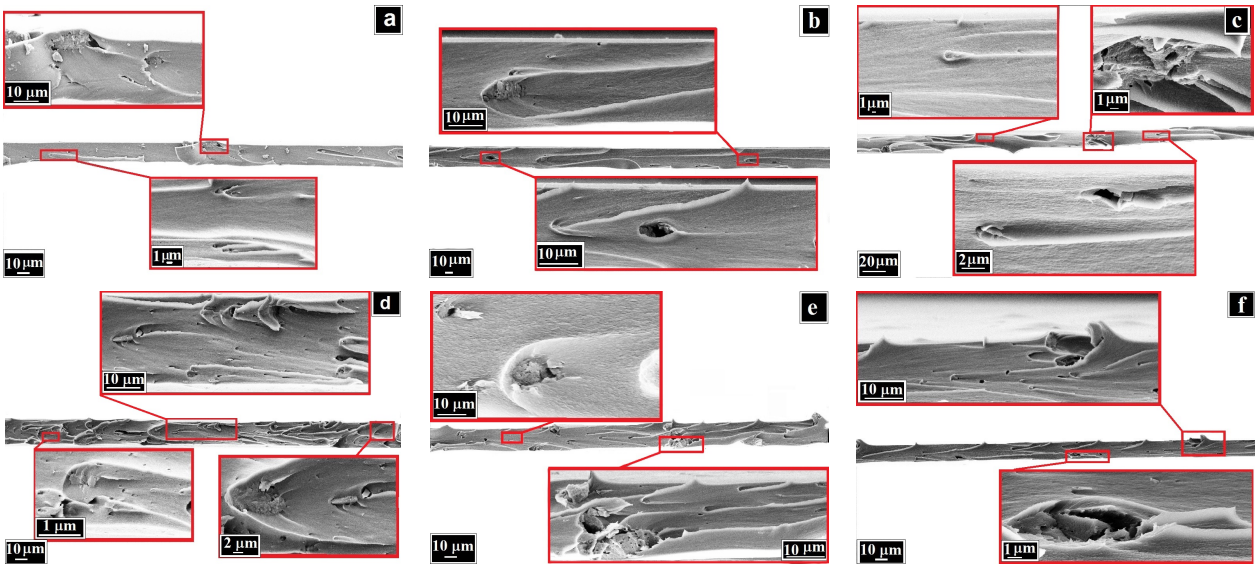

FIG. 6. SEM micrographs of the cryo-fractured surfaces of PMDA-ODA polyimide composites with different fillers and concentrations: 0.5 vol.% FLG-1 (a), 0.5 vol.% FLG-2 (b), 0.5 vol.% FLG-3 (c), 2 vol.% FLG-1 (d), 2 vol.% FLG-2 (e), 2 vol.% FLG-3 (f)

TABLE 5. Dielectric characteristics of PMDA-ODA matrix films and PMDA-ODA-based composite materials

Sample	ρ_V, Ω·m	ρ_s, Ω
PMDA-ODA	4.64E+13	1.03E+10
PMDA-ODA+0.5 vol. % FLG-0	1.67E+05	8.62
PMDA-ODA+2 vol. % FLG-0	3.96E+04	117
PMDA-ODA+0.5 vol. % FLG-1	2.12E+13	6.90E+09
PMDA-ODA+2 vol. % FLG-1	3.84E+12	1.21E+09
PMDA-ODA+0.5 vol. % FLG-2	2.71E+12	5.86E+08
PMDA-ODA+2 vol. % FLG-2	1.96E+12	5.86E+08
PMDA-ODA+0.5 vol. % FLG-3	3.23E+13	9.66E+09
PMDA-ODA + 2 vol. % FLG-3	5.12E+10	3.10E+07

4. Conclusions

Comprehensive studies have demonstrated the potential of introducing synthesized 2D graphene structures obtained from various biopolymers into the PMDA-ODA polymer matrix as a method for preparing new composite materials.

It was established that the most significant change in Young's modulus (by 11 %) of the film material was recorded with the introduction of 2 vol. % FLG-1, derived from lignin. Similar, albeit less pronounced, changes in the mechanical properties of PI are observed with the introduction of FLG obtained from cellulose and starch.

Incorporating synthesized nanoparticles into the PMDA-ODA PI matrix significantly affects the thermal characteristics of the film materials. Although a decrease in thermal stability was observed in all cases, the effect on the glass transition temperature was ambiguous. For instance, the introduction of 2 vol. % FLG-3, synthesized from cellulose, increased the glass transition temperature by 11 °C, while in other cases, a decrease was recorded. It is also worth noting that introducing synthesized nanoparticles into the PMDA-ODA matrix did not significantly reduce volume and surface resistivity in any of the cases considered.

Thus, the results of this study have shown that the degree of change in the properties of the polymer material significantly depends on the nature of the biopolymer from which the FLG was synthesized. This opens new opportunities for developing and optimizing polyimide film materials with specified characteristics for various engineering fields, including protective dielectric films and coatings. Further research in this area may lead to a deeper understanding of the interaction mechanisms between components and contribute to creating materials with tailored properties.

References

[1] Bessonov M.I., Koton M.M., Kudryavtsev V.V. Laius L.A. *Polyimides – Thermally Stable Polymers*. New York: Plenum Publishing Corp., 1987, 374 p.

[2] Ha C.-S., Mathews A.S. Polyimides and high performance organic polymers. *Advanced Functional Materials*, 2011, P. 1–36.

[3] Sezer Hicyilmaz A., Celik Bedeloglu A. Applications of polyimide coatings: a review. *SN Applied Sciences*, 2021, **3** (3), P. 1–22.

[4] Paul D.R., Robeson L.M. Polymer nanotechnology: nanocomposites. *Polymer*, 2008, **49** (15), P. 3187–3204.

[5] Jabeen S., Kausar A., Muhammad B., Gul S., Farooq M. A review on polymeric nanocomposites of nanodiamond, carbon nanotube, and nanobifiller: structure, preparation and properties. *Polymer-Plastics Technology and Engineering*, 2015, **54** (13), P. 1379–1409.

[6] Rizvanova P.G., Magomedov G.M., Kozlov G.V., Dolbin I.V. Local and spatial structure of nanofiller in polymer matrix and its influence on the properties of nanocomposites. *Inorganic Materials: Applied Research*, 2020, **11**, P. 665–668.

[7] Khlebtsov B.N. Functional nanoparticles: synthesis and practical applications. *Colloid Journal*, 2023, **85** (4), P. 475–478.

[8] Gudkov M.V., Stolyarova D.Y., Shiyanova K.A., Mel'nikov V.P. Polymer composites with graphene and its derivatives as functional materials of the future. *Polymer Science, Series C*, 2022, **64** (1), P. 40–61.

[9] Larin S.V., Glova A.D., Serebryakov E.B., Nazarychev V.M., Kenny J.M., Lyulin S.V. Influence of the carbon nanotube surface modification on the microstructure of thermoplastic binders. *RSC advances*, 2015, **5** (64), P. 51621–51630.

[10] Lyulin S.V., Larin S.V., Nazarychev V.M., Fal'kovich S.G. Kenny J.M. Multiscale computer simulation of polymer nanocomposites based on thermoplastics. *Polymer Science, Series C*, 2016, **58**, P. 2–15.

[11] Falkovich S.G., Nazarychev V.M., Larin S.V., Kenny J.M., Lyulin S.V. Mechanical properties of a polymer at the interface structurally ordered by graphene. *The Journal of Physical Chemistry C*, 2016, **120** (12), P. 6771–6777.

[12] Akinwande D., Brennan C.J., Bunch J.S., Egberts P., Felts JR, Gao H, et al. A review on mechanics and mechanical properties of 2D materials – Graphene and beyond., Extreme Mechanics Letters. *Elsevier Ltd*, 2017, **13**, P. 42–77.

[13] Saha J.K., Dutta A. A review of graphene: material synthesis from biomass sources, waste and biomass valorization. Springer Netherlands, 2022, **13**, P. 1385–1429.

[14] Fazil S., Bangesh M., Rehman W., Liaqat K., Saeed S., Sajid M., Waseem M., Shakeel M., Bibi I., Guo C.Y. Mechanical, thermal, and dielectric properties of functionalized graphene oxide/polyimide nanocomposite films. *Nanomaterials and Nanotechnology*, 2019, **9**, P. 1–8.

[15] Huang T., Xin Y., Li T., Nutt S., Su C., Chen H., Liu P., Lai Z. Modified graphene/polyimide nanocomposites: reinforcing and tribological effects. *ACS applied materials & interfaces*, 2013, **5** (11), P. 4878–4891.

[16] Li D., Yang W., Chen Y., Xiao C., Wei M. Effect of modified graphene on thermal, mechanical and tribological performance of polyimide based composites. *Materials Research Express*, 2018, **5** (6), 065304.

[17] Ogbonna V.E., Popoola P.I., Popoola O.M., Adeosun S.O. A review on recent advances on improving polyimide matrix nanocomposites for mechanical, thermal, and tribological applications: Challenges and recommendations for future improvement. *Journal of Thermoplastic Composite Materials*, 2023, **36** (2), P. 836–865.

[18] Liu P, Yao Z, Zhou J. Mechanical, thermal and dielectric properties of graphene oxide/polyimide resin composite. *High Performance Polymers*, 2016, **28** (9), P. 1033–1042.

[19] Tayouri M.I., Estaji S., Mousavi S.R., Salkhi Khasraghi S., Jahanmardi R., Nouranian S., Arjmand M., Khonakdar H.A. Degradation of polymer nanocomposites filled with graphene oxide and reduced graphene oxide nanoparticles: A review of current status. *Polymer Degradation and Stability*, 2022, **206**, 110179.

[20] Voznyakovskii A, Vozniakovskii A, Kidalov S. New way of synthesis of few-layer graphene nanosheets by the self-propagating high-temperature synthesis method from biopolymers. *Nanomaterials*, 2022, **12** (4), 657.

[21] Neverovskaya A.Y., Voznyakovskii A.P., Krupskaya L.T., Shugalei I.V., Vozniakovskii A.A. Conifer Bark as a Precursor of 2D Graphene Structures: Synthesis and Application. *Russian Journal of General Chemistry*, 2023, **93** (13), P. 3474–3482.

[22] Voznyakovskii A.P., Karmanov A.P., Neverovskaya A.Y., Vozniakovskii A.A., Kocheva L.S., Kidalov S.V. Biomass of Sosnowsky's hogweed as raw material for obtaining 2d carbonic nanostructures. *Russian Journal of Bioorganic Chemistry*, 2021, **47** (7), P. 1381–1388.

[23] Merzhanov A.G. The chemistry of self-propagating high-temperature synthesis. *Journal of Materials Chemistry*, 2004, **14** (12), P. 1779–1786.

[24] Zaaba N.I., Foo K.L., Hashim U., Tan S.J., Liu W.W., Voon C.H. Synthesis of graphene oxide using modified hummers method: solvent influence. *Procedia Engineering*, 2017, **184**, P. 469–477.

[25] Stone A.J., Wales D.J. Theoretical studies of icosahedral C60 and some related species. *Chemical Physics Letters*, 1986, **128** (5–6), P. 501–503.

[26] Kuntsman I., Nikolaeva A., Didenko A., Vlasova E., Ivan'kova E., Gofman I., Larin S. The role of carbon nanofillers in the aging processes of polyimide composites. *Journal of Polymer Research*, 2025, **32** (6), 223.

[27] Nikolaeva A.L., Bugrov A.N., Sokolova M.P., Ivan'kova E.M., Abalov I.V., Vlasova E. N., Gofman I.V. Metal oxide nanoparticles: an effective tool to modify the functional properties of thermally stable polyimide films. *Polymers*, 2022, **14** (13), 2580.

[28] Voznyakovskii A.P., Neverovskaya A.Y., Gorelova E.V., Zabelina A.N. Facile synthesis of 2D carbon structures as a filler for polymer composites. *Nanosystems: Physics, Chemistry, Mathematics*, 2018, **9** (1), P. 125–128.

[29] Richardson S., Gorton L. Characterisation of the substituent distribution in starch and cellulose derivatives. *Analytica Chimica Acta*, 2003, **497** (1–2), P. 27–65.

[30] Li J., Li Y., Wu Y., Zheng M. A comparison of biochars from lignin, cellulose and wood as the sorbent to an aromatic pollutant. *Journal of hazardous materials*, 2014, **280** (15), P. 450–457.

[31] Podlozhnyuk N., Vozniakovskii A., Kidalov S., Voznyakovskii A. Performance properties of epoxy resin modified with few-layer graphene obtained by the method of self-propagating high-temperature synthesis. *Polymers*, 2025, **17** (6), 812.

[32] Huang L., Zhang D., Zhang F.H., Feng Z.H., Huang Y.D., Gan Y. High-contrast SEM imaging of supported few-layer graphene for differentiating distinct layers and resolving fine features: there is plenty of room at the bottom. *Small*, 2018, **14** (22), 1704190.

[33] Kim J., Kim F., Huang J. Seeing graphene-based sheets. *Materials Today*, 2010, **13** (3), P. 28–38.

[34] Scardaci V., Compagnini G. Raman spectroscopy investigation of graphene oxide reduction by laser scribing. *Journal of Carbon Research*, 2021, **7** (2), 48.

[35] Johra F.T., Lee J.W., Jung W.G. Facile and safe graphene preparation on solution based platform. *Journal of Industrial and Engineering Chemistry*, 2014, **20** (5), P. 2883–2887.

[36] Stobinski L., Lesiak B., Malolepszy A., Mazurkiewicz M., Mierzwa B., Zemek J., Jiricek P., Bieloshapka I. Graphene oxide and reduced graphene oxide studied by the XRD, TEM and electron spectroscopy methods. *Journal of Electron Spectroscopy and Related Phenomena*, 2014, **195**, P. 145–154.

[37] Buhler K-U. *Spezialplaste*. Berlin: Academie. Verlag, 1978, 1015 p.

[38] Ioni Y.V., Sapkov I.V., Chentsov S.I., Efremova E.I., Gubin S.P. New method for preparation of composite based on montmorillonite and graphene oxide. *Russian Journal of Inorganic Chemistry*, 2023, **68** (4), P. 487–495.

[39] Gofman I.V., Abalov I.V., Yudin V.E., Tiranov V.G. Mechanical and thermal properties of nanocomposite films based on an aromatic polyimide and carbon nanocones. *Physics of the Solid State*, 2011, **53**, P. 1509–1515.

[40] Kamalov A., Didenko A., Ivanov A., Kodolova-Chukhontseva V., Terebova N., Ivan'kova E., Popova E., Yudin, V. Effect of the rigidity of polyimide matrices on the electrical conductivity of graphene-containing composites. *Journal of Polymer Research*, 2025, **32** (1), P. 1–13.

[41] Smirnova V.E., Gofman I.V., Ivan'kova E.M., Didenko A.L., Krestinin A.V., Zvereva G.I., Yudin V.E.. Effect of single-walled carbon nanotubes and carbon nanofibers on the structure and mechanical properties of thermoplastic polyimide matrix films. *Polymer Science Series A*, 2013, **55**, P. 268–278.

[42] Guadagno L., De Vivo B., Di Bartolomeo A., Lamberti P., Sorrentino A., Tucci V., Vertuccio L., Vittoria V. Effect of functionalization on the thermo-mechanical and electrical behavior of multi-wall carbon nanotube/epoxy composites. *Carbon*, 2011, **49** (6), P. 1919–1930.

Submitted 14 February 2025; revised 13 November 2025; accepted 13 December 2025

Information about the authors:

Elena N. Bykova – Branch of Petersburg Nuclear Physics Institute named by B.P. Konstantinov of National Research Centre "Kurchatov Institute" – Institute of Macromolecular Compounds, Bolshoi, 31, St. Petersburg, 199004 Russia; ORCID 0000-0002-3774-6792; bykova.elena.n@gmail.com

Iosif V. Gofman – Branch of Petersburg Nuclear Physics Institute named by B.P. Konstantinov of National Research Centre "Kurchatov Institute" – Institute of Macromolecular Compounds, Bolshoi, 31, St. Petersburg, 199004 Russia; ORCID 0000-0002-1939-2660; gofman@imc.macro.ru

Igor V. Kuntsman – Branch of Petersburg Nuclear Physics Institute named by B.P. Konstantinov of National Research Centre "Kurchatov Institute" – Institute of Macromolecular Compounds, Bolshoi, 31, St. Petersburg, 199004 Russia; ORCID 0000-0002-4535-0560; i.v.kuntsman@gmail.com

Elena M. Ivan'kova – Branch of Petersburg Nuclear Physics Institute named by B.P. Konstantinov of National Research Centre "Kurchatov Institute" – Institute of Macromolecular Compounds, Bolshoi, 31, St. Petersburg, 199004 Russia; ORCID 0000-0002-4823-0695; ivelen@mail.ru

Alexandr P. Voznyakovskii – Lebedev Institute of Synthetic Rubber, Gapsal'skaya, 1, St. Petersburg, 198035 Russia; ORCID 0000-0002-5979-3661; voznap@mail.ru

Aleksei A. Vozniakovskii – Ioffe Institute, Polytekhnicheskaya, 26, St. Petersburg, 194021 Russia; ORCID 0000-0001-6482-172X; alexey_inform@mail.ru

Anna Yu. Neverovskaya – Lebedev Institute of Synthetic Rubber, Gapsal'skaya, 1, St. Petersburg, 198035 Russia; ORCID 0000-0001-7813-666X; anna-neverovskaya@yandex.ru

Conflict of interest: the authors declare no conflict of interest.